*J. Fluid Mech.* (1979), *vol.* 94, *part* 3, *pp.* 561–576
*Printed in Great Britain*

# Turbulent diffusion and degradation of polymer molecules in a pipe and boundary layer

By L. I. SEDOV, V. A. IOSELEVICH, V. N. PILIPENKO AND N. G. VASETSKAYA

Institute of Mechanics, Moscow State University

(Received 14 November 1977)

Results from a series of pipe-flow experiments using a range of water-soluble drag-reducing polymers are presented. Degradation has been investigated by means of multiple passes of the solutions through a pipe. A theory predicting drag reduction in pipe flow has been devised which agrees with the experimental results. Changes in polymer molecular weight due to degradation are taken into account. The analysis is then applied to a turbulent boundary layer with polymer injection.

## 1. Introduction

The practical use of drag-reducing polymer additives is restricted by wall roughness and degradation. The influence of roughness on reduction has been studied experimentally (Vasetskaya & Ioselevich 1970; Spangler 1969; Virk 1971; Ivanuta & Chekalova 1976). Drag reduction was found in the transition regime and in the case hydraulically smooth walls. In the 'fully rough' regime polymer additives have no significant influence. In the transition regime additives can cause a larger friction reduction than near hydraulically smooth walls. The transition and 'fully rough' regimes occur at higher Reynolds numbers. There are schemes for calculating the drag reduction for rough walls (Vasetskaya & Ioselevich 1970; Ioselevich & Pilipenko 1973; Poreh 1970). The results of these calculations agree with the experiments.

The study of mechanical degradation involves, generally speaking, the determination of relations between the probability of breaking of molecular chains, the strength of chemical bonds and the intensity of external forces. However, present knowledge about turbulence structure and macromolecule configurations in fluid flows is limited, which is a great obstacle to a study of this kind. The available experimental data allow a phenomenological analysis.

Degradation in turbulent shear flows has previously been studied experimentally (Gramain & Philippides 1975; Ram Arie 1975; Kim *et al.* 1974; van der Meulen 1974; Gulter, Zakin & Patterson 1975; Block Moran & Walker 1974; Sellin 1974). The degradation was found to vary for different polymer solutions. The rate of degradation increases with the mean molecular weight (Gramain & Philippides 1975), while branched-chain macromolecules have a greater mechanical strength (Kim *et al.* 1974). The polymer 'impotence' also grows with the decreasing polymer concentration (van der Meulen 1974). Some experiments have examined the influence of polymer concentration and wall shear stress on the way the viscosity of the solution changes during degradation (Ram Arie 1975). A threshold of the wall shear stress has been

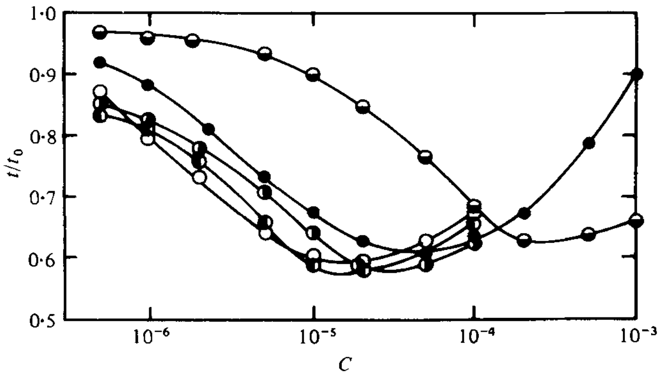

FIGURE 1. The efficiency of polymer solutions as a function of concentration at a temperature 16–18 °C, $\Delta p$ = 80 kNm$^{-2}$. ●, PEO; ○, P-97; ◑, P-75; ◐, P-939; ⊖, GG.

found. Degradation is not observed in laminar tube flow if the wall stress is less than this threshold (Gulter *et al.* 1975). However, in laminar pipe flow degradation takes place chiefly in the entry region, where the wall stress is highest. In turbulent flow degradation is observed both in the entry region and in the fully developed flow (Gulter *et al.* 1975). The experimental data show that degradation is more intense in turbulent flow than in laminar flow.

The quantitative prediction of mechanical degradation requires a kinetic equation for the mean polymer molecular weight. A possible version of this phenomenological equation was suggested earlier (Sedov, Ioselevich & Pilipenko 1977). A first approximation to the values of certain parameters was deduced from the available data, but further experiments were necessary. These experiments have now been carried out at the Institution of Mechanics, Moscow State University. The new results allow an analysis of the influence of the polymer concentration, mean molecular weight, wall stress, temperature, wall roughness and pipe entry conditions. The corrected kinetic equation for the mean molecular weight is applied to a turbulent boundary layer on a plate.

## 2. Experiments

The experiments were conducted with dilute solutions of polyethylene oxide (PEO, molecular weight $M \simeq 3 \times 10^6$), polyacrylamides (types P-75, P-939, P-97, with $M \simeq 10^7$) and guar gum.

Immediately after the preparation of the solutions the drag-reducing efficiency of the polymer solutions was determined by a single pass through a smooth tube of length 1·50 m and diameter 0·39 cm at a pressure drop $\Delta p$ = 80 kNm$^{-2}$. This pressure drop was not high enough to cause degradation. The efficiency of the polymer solutions was defined as the ratio $t/t_0$, where $t$ is time required for a fixed volume $V_0$ of solution to pass through the tube and $t_0$ the time for an equal volume of water. The control experiments were performed with concentrations ranging from $5 \times 10^{-7}$ to $10^{-3}$ at a temperature of 16–18 °C. The data are given in figure 1. The ratio $t/t_0$ has a minimum as a function of the concentration. The minimum value $(t/t_0)_{\min}$ varied little for the different polymers (between 0·58 and 0·62), polyacrylamide being slightly more

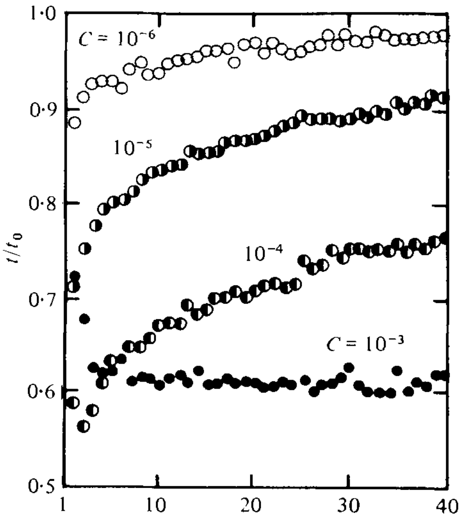

FIGURE 2. The degradation of polyethylene oxide solutions at $\Delta p = 500\ \mathrm{kNm^{-2}}$ (PEO).

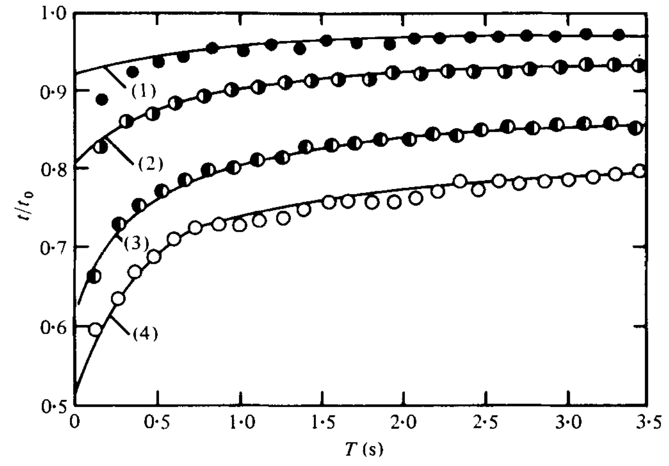

FIGURE 3. The degradation of polyethylene oxide solutions at $\Delta p = 400\ \mathrm{kNm^{-2}}$. (1) $A = 1{\cdot}4 \times 10^{-19}\ \mathrm{s\,m^{-2}}$; (2) $A = 5{\cdot}0 \times 10^{-19}\ \mathrm{s\,m^{-2}}$; (3) $A = 2{\cdot}2 \times 10^{-19}\ \mathrm{s\,m^{-2}}$; (4) $A = 1{\cdot}2 \times \times 10^{-19}\ \mathrm{s\,m^{-2}}$. ●, $C = 10^{-6}$; ◑, $C = 3 \times 10^{-6}$; ◐, $C = 10^{-5}$; ○, $C = 3 \times 10^{-5}$.

effective, followed by polyethylene oxide and then guar gum. Polyacrylamide was probably more effective because it has a high molecular weight. The cause of the decrease in drag-reduction efficiency at higher concentrations is probably the increase in the viscosity of the solution with the growth of interaction between the macromolecules.

Degradation was studied by means of multiple passes through a pipe (length 1·50 m, diameter 0·39 cm, smooth entry). Each series of tests was performed with a constant pressure drop $\Delta p$. The duration $t_n$ of the $n$th pass of a fixed liquid volume $V_0$ was measured, the solution temperature being maintained between 15 and 18 °C. Figure 2 shows the results for polyethylene oxide solutions at $\Delta p = 500\ \mathrm{kN^{-2}}$. The degradation

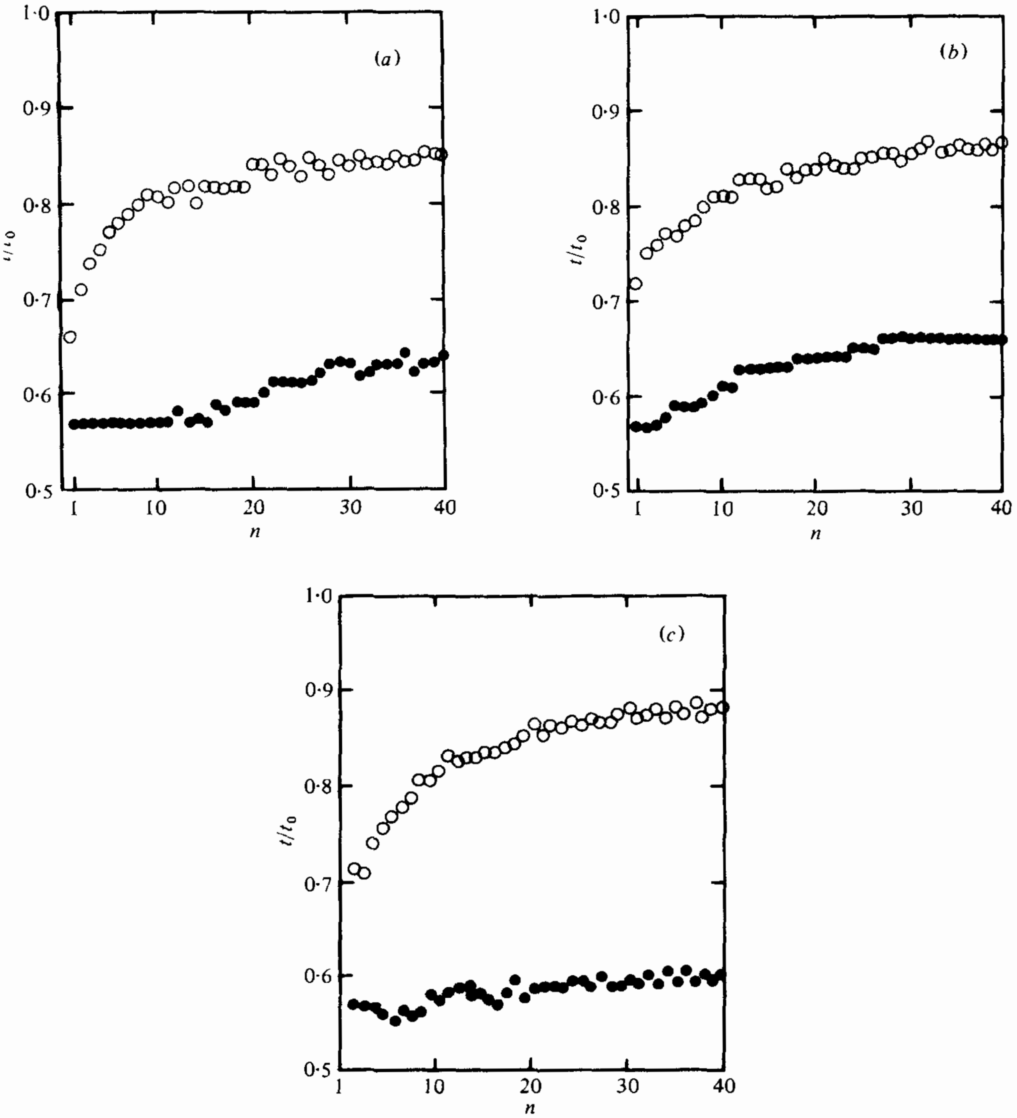

FIGURE 4. The degradation of polyacrylamide solutions at $\Delta p = 500\,\mathrm{kNm}^{-2}$. ○, $C = 10^{-5}$; ●, $C = 10^{-4}$, (*a*) P-97; (*b*) P-75; (*c*) P-939.

of these polymer solutions is intense, e.g. when the concentration $C = 10^{-5}$ the value of $t/t_0$ varies from 0·7 to 0·9 for 40 passes, which is equivalent to a change in drag reduction from 50 to 20 %. When $C > C_{\mathrm{opt}}$, $t/t_0$ decreases in the initial stage of the degradation process. Figure 3 shows the results of similar series of experiments with polyethylene oxide solutions at $\Delta p = 400\,\mathrm{kN\,m}^{-2}$.

The data for polyethylene solutions ($C = 10^{-5}$ and $10^{-4}$) are given in figures 4(*a*), (*b*) and (*c*). These tests were carried out at $\Delta p = 500\,\mathrm{kN\,m}^{-2}$. In spite of a higher molecular weight, the degradation rates of these polymers are less than that of polyethylene oxide. Figure 5 shows the experimental data for guar gum solutions. Their efficiency was unaffected by 40 passes. This agrees with Naudascher (1972).

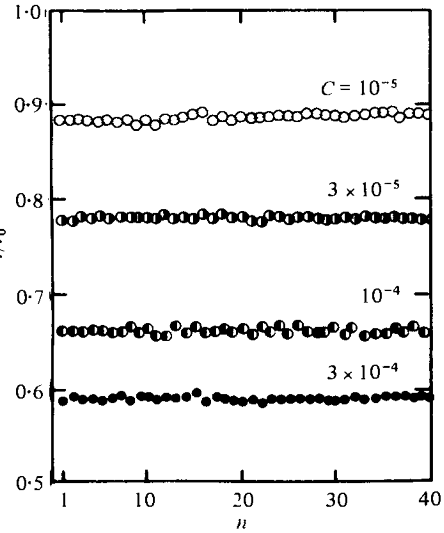

FIGURE 5. The degradation of guar gum solutions at $\Delta p$ = 500 kNm$^{-2}$ (GG).

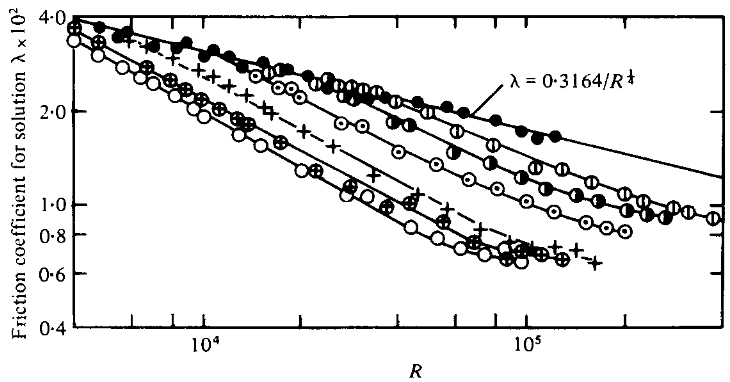

FIGURE 6. The influence of temperature on the efficiency of polyethylene oxide solutions with $C = 10^{-5}$. ⦶, $\theta$ = 70 °C; ◑, $\theta$ = 50 °C; ⊙, $\theta$ = 30 °C; +, $\theta$ = 20 °C, ⊕, $\theta$ = 10° C; ○, $\theta$ = 2 °C; ●, water.

The effect of temperature was studied with polyethylene oxide solutions ($C = 10^{-5}$) in a smooth pipe (length 2·0 m, diameter 0·9 cm) with a pressure drop of 10–500 kNm$^{-2}$. The temperature varied from 2 to 70 °C. Figure 6 shows the influence of temperature on drag reduction for a single pass of a fresh solution which suffers negligible degradation. As the temperature increases the Reynolds number $R_0$ for the onset of drag reduction increases. At the same value of the ratio of the wall stress $\rho V_*^2$ to the wall stress $\rho (V_*^0)^2$ at the onset of drag reduction, the efficiency of polymers decreases as the temperature increases. The degradation rate also increases with temperature. This was observed in experiments with polyethylene oxide solutions ($C = 10^{-5}, \Delta p$ = 500kNm$^{-2}$, pipe diameter = 0·39 cm, pipe length = 1·50 m), as shown in figure 7.

The influence of wall shear stress on the degradation rate can be seen in figure 8, where the results of experiments with polyethylene oxide solutions ($C = 10^{-5}$) at $\Delta p$ = 100, 200 and 400 kNm$^{-2}$ are given.

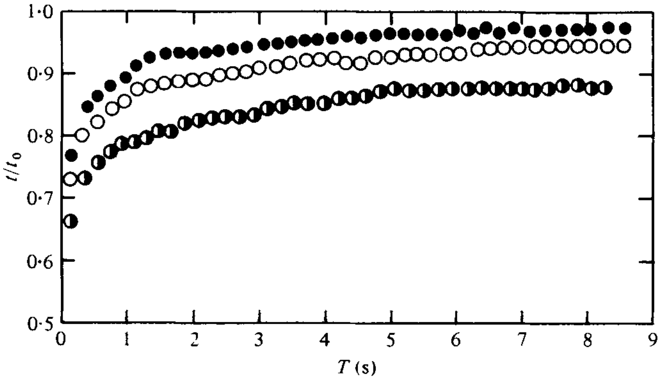

FIGURE 7. The degradation of polyethylene oxide solutions at different temperatures. ●, $\theta$ = 50 °C; ○, $\theta$ = 23 °C; ◑, $\theta$ = 9 °C.

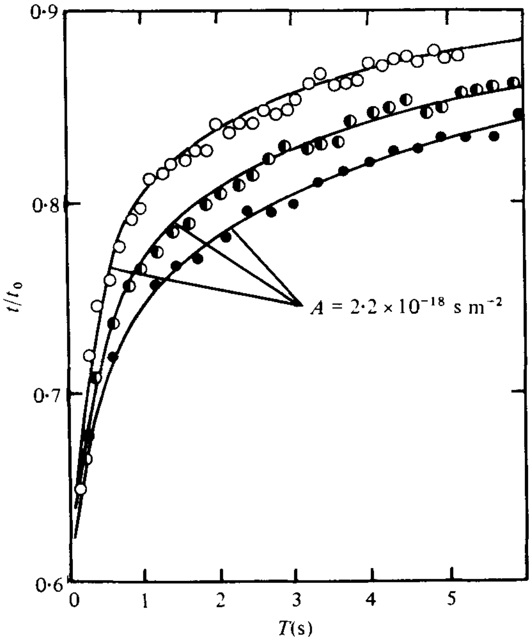

FIGURE 8. The influence of wall shear stress on the degradation of polyethylene oxide solutions with $C = 10^{-5}$. ○, $\Delta p$ = 400 kNm$^{-2}$; ◐, $\Delta p$ = 200 kNm$^{-2}$; ●, $\Delta p$ = 100 kNm$^{-2}$.

A series of experiments with polyethylene oxide solutions was carried out in rough tube (length 1·50 m, diameter 0·4 cm). The roughness took the form of an inside thread of triangular profile 0·5 mm high. A solution ($C = 10^{-5}$) was repeatedly passed through the pipe at $\Delta p$ = 500 kNm$^{-2}$. The first pass was the quickest, while the second pass was the slowest. Subsequent passes gradually shortened to the time for pure water. According to Vasetskaya & Ioselevich (1970) and Ioselevich & Pilipenko (1973), the first pass has a Reynolds number near the upper limit of the roughness transition regime. Through degradation the drag-reduction efficiency drops and this upper limit is displaced to lower Reynolds numbers. All subsequent passes took place in the 'fully rough' regime, where the drag of polymer solutions slightly exceeded

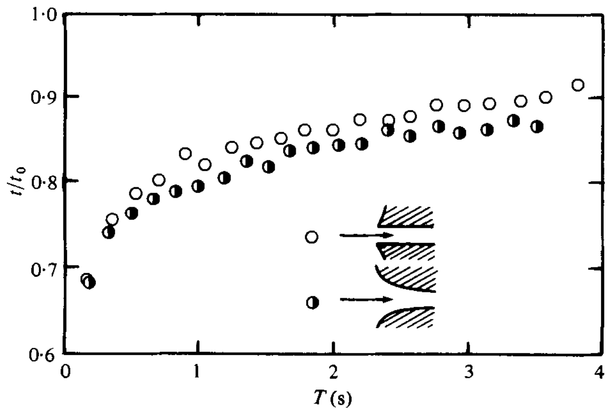

FIGURE 9. The effect of a sharp edge in the pipe entry.

(by 6–8 %) the drag of pure water. This excess gradually vanished through further degradation. It is found that the degradation rate in the rough pipe was ten times greater than that in a smooth pipe with the same diameter at the same pressure drop.

Figure 9 shows the effect of a pipe entry with a sharp edge. The tests were run with polyethylene oxide solutions ($C = 10^{-5}$) in a smooth pipe at $\Delta p = 300\ \mathrm{kNm}^{-2}$.

## 3. Drag reduction

To analyse the experimental data is was necessary to refine the theory proposed in Vasetskaya & Ioselevich (1970) and Sedov *et al.* (1974). Recent measurements of velocity profiles have shown that those used in these papers were insufficiently accurate in the buffer zone near the wall, leading to higher friction coefficients. A more precise expression for the mixing length is (Pilipenko 1975; Sedov, Ioselevich & Pilipenko 1977)

$$l = l_1[1-\exp(-A_0 l_0 F\eta)], \tag{3.1}$$

where
$$l_1 = a[0{\cdot}14\text{–}0{\cdot}08(1-\eta/\eta_a)^2 - 0{\cdot}06(1-\eta/\eta_a)^4],$$
$$l_0 = \psi^{\frac{1}{2}}e(\psi), \quad \psi = 1-\eta_a^*/\eta_a,$$
with
$$\eta = yV_*/\nu, \quad \eta_a = aV_*/\nu, \quad \eta_a^* = (2R_*)^{\frac{1}{2}}.$$

Here $e$ is the Heaviside step-function, $a = \frac{1}{2}d$ is the radius of the tube, $R_*$ is the Reynolds number at transition from laminar to turbulent flow, and $A_0 = 0{\cdot}0385$. The efficiency of the different polymers will be characterised by $F$ in (3.1), whose form we propose should be

$$F = 1-f_1(C, M)f_2(V_*/V_*^0). \tag{3.2}$$

In the polyethylene oxide experiments we find that the drag reduction is a maximum at $V_*/V_*^0 \approx 10$ while for $V_*/V_*^0 > 10$ the effect of the polymer additives is independent of $V_*/V_*^0$; we thus take $f_2 = 1$ for $V_*/V_*^0 \geqslant 10$. Also, polymer additives give no drag reduction for $V_*/V_*^0 \leqslant 1$, so we take $f_2 = 0$ for $V_*/V_*^0 \leqslant 1$. The drag-reduction maximum has been associated with the combination $CM^{0{\cdot}85}$ (Vasetskaya & Ioselevich 1970; Sedov *et al.* 1974), so we assume in (3.2) that $f_1 = f_1(CM^{0{\cdot}85})$. Figure 10 shows the observed relation between the reduction in the friction coefficient and the

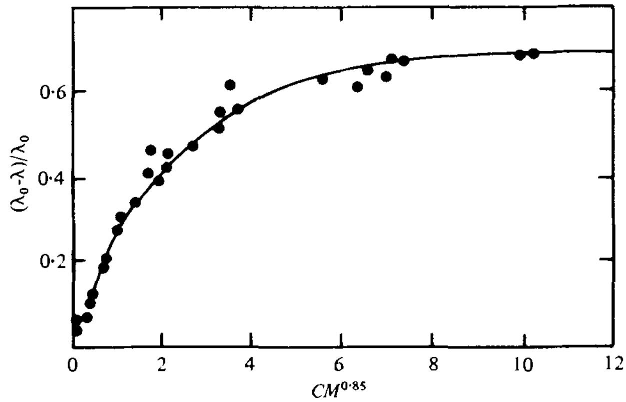

FIGURE 10. The relation between the reduction in the friction coefficient and the parameter $CM^{0\cdot 85}$. The solid line is the result of integration of the Reynolds equation at $f_2 = 1$.

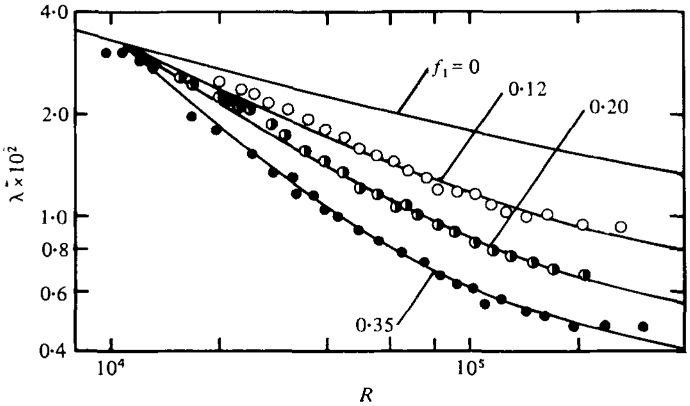

FIGURE 11. The friction coefficient *versus* Reynolds number, the solid line is the result of integration. PEO, $d = 3\cdot 21$ cm. ○, $C = 5\times 10^{-6}$; ◑, $C = 2\times 10^{-5}$; ●, $C = 10^{-4}$.

parameter $CM^{0\cdot 85}$ (Hoyt 1966), which can be converted into a relation between $F$ and $CM^{0\cdot 85}$ by Reynolds equation:

$$[1+(lV_*/\nu)^2\xi]\,\xi = 1-\eta/\eta_a, \quad \xi = du^+/d\eta, \quad u^+ = u/V_*. \tag{3.3}$$

The solid line in figure 10 is the result of integrating with $f_2 = 1$ (the maximum friction reduction) and $R = 1\cdot 4\times 10^4$ and using the empirical approximation

$$f_1 = 0\cdot 58\tan^{-1}(1\cdot 2\,CM^{0\cdot 85}).$$

Satisfactory agreement with the experiments (Virk *et al.* 1967) is obtained with the empirical approximation (see figure 11)

$$f_2 = (2/\pi)\tan^{-1}[1\cdot 7(V_*/V_*^0-1)]\,e(V_*/V_*^0-1).$$

Thus our final form for $F$ is

$$F = 1-0\cdot 37\tan^{-1}[1\cdot 7(V_*/V_*^0-1)]\tan^{-1}(1\cdot 2\,CM^{0\cdot 85}). \tag{3.4}$$

Outside the wall layer the logarithmic law is applicable:

$$u^+ = \kappa^{-1}\ln\eta + B. \tag{3.5}$$

Our parameter $F$ in (2.1) is related to the constant $B$ in (3.5) through

$$B = (8{\cdot}8/F^{0{\cdot}6}) - 3{\cdot}3. \tag{3.6}$$

We now turn to the onset friction velocity $V_*^0$. There are two hypotheses which relate $V_*^0$ to the molecular characteristics (Virk *et al.* 1966; Virk & Merrill 1969; Lumley 1969; Hoyt 1972; Virk 1975). According to the first hypothesis, the polymer molecules cause drag reduction when their radius of gyration $l_m$ is comparable with the characteristic length scale of the turbulence, i.e.

$$l_m V_*^0/\nu = R_m^0, \quad \text{a constant.} \tag{3.7}$$

Now the typical size of a macromolecule in a stationary solvent is related to the molecular weight by $l_m \simeq 1{\cdot}9\times 10^{10} M^{0{\cdot}5}$m, so that we find from our experimental data that $R_m^0 \approx 0{\cdot}01$ (Vasetskaya & Ioselevich 1970). Thus the polymer molecules first cause drag reduction when they are very much smaller than the length scale of the turbulent flow, so the first hypothesis cannot be true. According to the second hypothesis drag reduction first occurs when the longest relaxation time of the polymer $t_m$ is comparable with the characteristic time scale of the turbulence $\nu/V_*^2$, i.e.

$$t_m(V_*^0)^2/\nu = t_0^+, \quad \text{a constant.} \tag{3.8}$$

Now the value of $t_m$ has been found from experiments and from analysis of the kinetics of molecular chains (e.g. see Shin 1965) to be given by

$$t_m = 6M\rho\nu[\mu]/\pi^2 R\theta_a,$$

in which $R$ is the universal gas constant, $\theta_a$ is the absolute temperature and $[\mu]$ is the intrinsic viscosity. Our experimental data then show that the value of $t_0^+$ is close to 1. Moreover, (3.8) is more accurate than (3.7) (Cox, North & Dunlop 1974; Berman & George 1974). Substituting an expression for $[\mu]$ (see Shin 1965), we obtain the following formula for $V_*^0$:

$$V_*^0 \approx E_0/M^{0{\cdot}89}, \quad E_0 \approx \text{constant.} \tag{3.9}$$

According to Virk (1975), the constant $E_0$ is $1{\cdot}37\times 10^4$ m/s for dilute solutions of polyethylene oxide at 18–22 °C. The temperature dependence of onset was found empirically for polyethylene oxide solutions to be

$$[V_*^0(\theta)]^2\,\nu(\theta) \simeq \text{constant.}$$

Our refined theory of drag reduction will consist of (3.1) together with (3.4) and (3.9), and will now be applied to analyse degradation.

## 4. Degradation in a pipe

We assume that the turbulent mixing is sufficiently intense for the molecular weight $M$ to vary little across the cross-section of the pipe. In Sedov *et al.* (1974) the rate of change of the mean molecular weight was assumed to take the form

$$dM/dt = -\alpha C^{-4} M^2 V_*^4, \tag{4.1}$$

where $\alpha$ should be a constant with units $s^3 m^{-4}$. In Sedov *et al.* (1974) an inaccurate velocity profile was used in the buffer layer, although $\alpha$ was found to be a constant for the few data then available. Analysis of the new experiments indicates some variation in $\alpha$. We thus tried a generalization of (4.1). In analogy with (4.1) let us assume

$$dM/dt = -A(C)\,M^m\,V_*^n, \tag{4.2}$$

with the exponents $m$ and $n$ and the function $A(C)$ to be found from the experiments. Solving (4.2) for fixed concentration and constant wall shear stress, we have

$$M(t) = [M_{(0)}^{1-m} - (1-m)\,A(0)\,V_*^n\,t]^{1/(1-m)}. \tag{4.3}$$

Although the mean molecular weight can be estimated by measuring the intrinsic viscosity (Shin 1965)

$$[\mu] = 1{\cdot}03\times 10^{-2}M^{0{\cdot}78}, \tag{4.4}$$

we found this method to be insufficiently accurate to measure the degradation in dilute solutions with $C < 10^{-4}$. This method did, however, give the initial molecular weight as $3\times 10^6$.

The alternative method we used to measure the molecular weight was to use its relationship with the drag reduction: the ratio of the flow times for equal volumes of solution and solvent at a constant pressure drop is

$$t/t_0 = \frac{\kappa^{-1}\ln\eta_a + 5{\cdot}5 - (3/2\kappa)}{\kappa^{-1}\ln\eta_a + B - (3/2\kappa)}. \tag{4.5}$$

The mean values $m = 4$ and $n = 2$ were found form correlation of the value of $t/t_0$ calculated from (3.4), (3.6) and (4.5) for $M(0) = 3\times 10^6$ with the experimental data shown in figure 8. The experimental results given in figure 3 and the values of the molecular weight, which were estimated by measuring (during the process of degradation) the intrinsic viscosity, indicated that $A(C)$ was approximately given by

$$A(C) = \begin{cases} 6\times 10^{-12}C^{1{\cdot}23} & \text{for}\quad C < 3\times 10^{-5}, \\ 3\times 10^{-22}C^{-1} & \text{for}\quad C \geqslant 3\times 10^{-5}, \end{cases} \tag{4.6}$$

$A$ having units $s\,m^{-2}$. Thus the rate of change of the mean molecular weight has been determined to be

$$dM/dt = -A(C)\,M^4\,V_*^2. \tag{4.7}$$

This expression differs from (4.1). The higher exponent for $M$ reflects the sensitivity of the degradation to the molecular weight which we found in our experiments. The polydispersity of the molecular weight is an important parameter in the kinetic equation, particularly if the exponent of the molecular weight is stated to be high. Therefore the kinetic equation (4.7) is approximate. The unusual form of the function $A(C)$ (at first increasing with $C$ and then decreasing) may be explained in terms of short-lived random bonds between the macromolecules formed in the turbulent mixing. At low values of $C$ the few random bonds which are formed per unit time cause a growth of the 'effective' molecular weight. Such 'extended molecules' are easily degraded. At higher concentrations the production of the random bonds increases and the degradation rate also grows. for At higher concentrations $C \geqslant 3\times 10^{-5}$ the individual macromolecules become closely packed (Lumley 1969), which causes very high production of random bonds with little overall degradation.

## 5. Degradation in a boundary layer

We now turn to the problem of a turbulent boundary layer on a flat plate with polymer additives injected near the leading edge, a problem in which degradation must be considered. Following Ioselevich & Pilipenko (1974), we assume that the concentration of drag-reducing polymers is related to the boundary-layer thickness $\delta$ and injection rate $q$ (volume flux per unit width of plate) by

$$C(x) \approx 2q\rho_p/U\delta(x)\rho, \tag{5.1}$$

where $x$ is the longitudinal co-ordinate, $U$ the velocity of the free stream, $\rho_p$ the density of injected polymer and $\rho$ the solution density. This formula is applicable when the polymer is injected near the leading edge, where a diffusion layer quickly develops. As in Ioselevich & Pilipenko (1973), we suppose that the injection imparts negligible momentum to the flow, so the polymers should not affect the flow outside the turbulent boundary layer.

Using the standard analogy between pipe flows and flat-plate boundary layers we can write down a kinetic equation similar to (4.7):

$$dM/dr = -A(C)\,M^4\,\omega^2\,\nu, \tag{5.2}$$

in which $\omega = (\frac{1}{2}C_f)^{\frac{1}{2}} = V_*/U$, with $C_f$ the local friction coefficient, $M$ is the cross-sectional mean value of the molecular weight, and $r = xU/\nu$ is the dimensionless longitudinal co-ordinate.

For the dimensionless velocity profile outside the wall layer we use (Ioselevich & Pilipenko 1973; Pilipenko 1977)

$$u^+ = \kappa^{-1}\ln\eta + B + \Pi\kappa^{-1}\,W(\eta/\eta_\delta), \tag{5.3}$$

with $$W(\eta/\eta_\delta) = 1-\cos(\pi\eta/\eta_\delta), \quad \eta_\delta = \delta V_*/\nu,$$

where $\Pi$ is the Coles parameter (in the absence of longitudinal pressure gradients $\Pi \approx 0{\cdot}55$) and $\kappa \simeq 0{\cdot}4$. $B$ is related to our drag-reduction parameter $F$ [see (3.4)] by

$$B = (8{\cdot}8/F^{0{\cdot}6}) - 3{\cdot}9, \tag{5.4}$$

which differs from (3.6) only by the different velocity 'defect'. From (5.4), (3.4) and (3.9) it follows that $B = \ = B(C, M, W)$. Differentiation (5.4) with respect to $r$ at $\eta = \eta_\delta$ and using $V_*\,u^+(\eta_\delta) = U$, a constant, yields

$$\frac{1}{\kappa\eta_\delta}\frac{d\eta_\delta}{dr} + \left(\frac{1}{\omega^2} + \frac{\partial B}{\partial \omega}\right)\frac{d\omega}{dr} + \frac{\partial B}{\partial M}\frac{dM}{dr} + \frac{\partial B}{\partial C}\frac{dC}{dr} = 0, \tag{5.5}$$

in which we may substitute

$$\frac{dC}{dr} = -2q^+\frac{\rho_p}{\rho\eta_\delta}\left(\frac{\omega}{\eta_\delta}\frac{d\eta_\delta}{dr} - \frac{d\omega}{dr}\right), \quad q^+ = q/\nu, \tag{5.6}$$

obtained from (5.1). Equations (4.2) and (4.5) together with the integral relation

$$\frac{(G_1 - G_2\,\omega)}{\eta_\delta}\frac{d\eta_\delta}{dr} - G_2\frac{d\omega}{dr} = \frac{\omega^2}{\eta_\delta}, \tag{5.7}$$

where $$G_1 = \kappa^{-1}(1+\Pi) \approx 3{\cdot}88, \quad G_2 = \kappa^{-2}(2+10\Pi/\pi + \tfrac{3}{2}\Pi^2) \approx 26{\cdot}26,$$

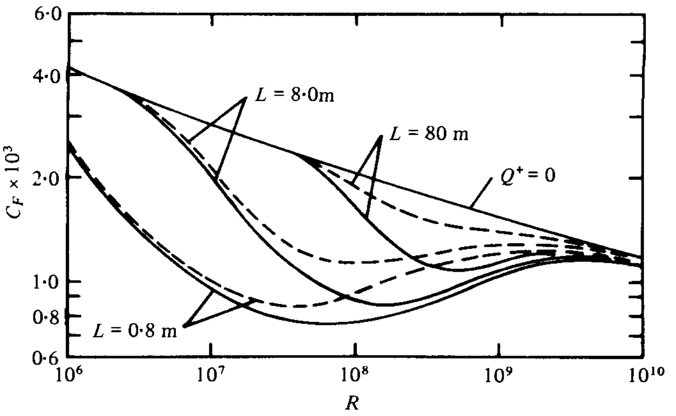

FIGURE 12. Theoretical results, $L$ is the plate length, the injection flux $Q^+ = 10$.

form the system of ordinary differential equations for $\eta_\delta(r)$, $\omega(r)$ and $M(r)$. The boundary conditions at the point of injection $r = r_0$ are obtained from the Blasius solution with the assumption that the injection imparts no momentum to the flow.

$$0{\cdot}664 r_0^{\frac{1}{2}} = [G_1 - G_2\,\omega(r_0)]\,\eta_\delta(r_0), \tag{5.8a}$$

$$1/\omega(r_0) = \kappa^{-1}\ln\eta_\delta(r_0) + 2\Pi\kappa^{-1} + B(C(r_0),\ M(r_0),\ \omega(r_0)), \tag{5.8b}$$

$$M(r_0) = M, \quad C(r_0) = 2q^+\rho_p\,\omega(r_0)/\rho\eta_\delta(r_0). \tag{5.8 c, d}$$

After determining the functions $\eta_\delta$, $\omega$ and $M$, it is possible to find the distribution of effective concentraton along the plate from (5.1). The total friction coefficient for a plate of length $L$ is then

$$C_F = \frac{2\eta_\delta(R)}{R}[G_1 - G_2\,\omega(R)] \quad \text{with} \quad R = \frac{LU}{\nu}. \tag{5.9}$$

Equations (5.2), (5.5) and (5.7) were integrated numerically (i) allowing for degradation and (ii) ignoring it. Calculations were made for plate lengths $L = 0{\cdot}8$, $8{\cdot}0$ and 80 m, various injection fluxes $Q^+ = 2q^+$ for both sides of the plate and $M_0 = 4 \times 10^6$.

Figure 12 shows the friction coefficient $C_F$ *vs.* the Reynolds number at $Q^+ = 10$. There is more degradation for the longer plates at the same $U$. For instance at $U = 20$ m/s the drag reduction is decreased through degradation by only 3 % for $L = 0{\cdot}8$ m (from 0·68 to 0·66), while for $L = 8$ m the decreases is 18 % (from 0·53 to 0·44) and for $L = 80$ m it is 84 % (from 0·18 to 0·03). At the injection rate studied the drag reduction is maximal for $L = 0{\cdot}8$ m, while for plates of length 8 m and 80 m maximum drag reduction is reached at $Q^+ = 100$ and 1000 respectively. The range of Reynolds numbers which give significant drag reduction decreases as the plate is lengthened and increases with increasing injection flux.

The influence of degradation on the drag reduction at different values of $Q^+$ is shown in figure 13 for a plate of length 8 m. At low $Q^+$ the effect is mainly at low velocities, while there is more degradation at high velocities for high $Q^+$.

The distributions of the mean molecular weight along a plate of length 8·0 m at $U = 20$ and 50 m/s, i.e. $R \approx 1{\cdot}5 \times 10^8$ and $3{\cdot}8 \times 10^6$, are shown in figures 14(*a*) and (*b*) for different injection fluxes, while the corresponding distributions of the effective

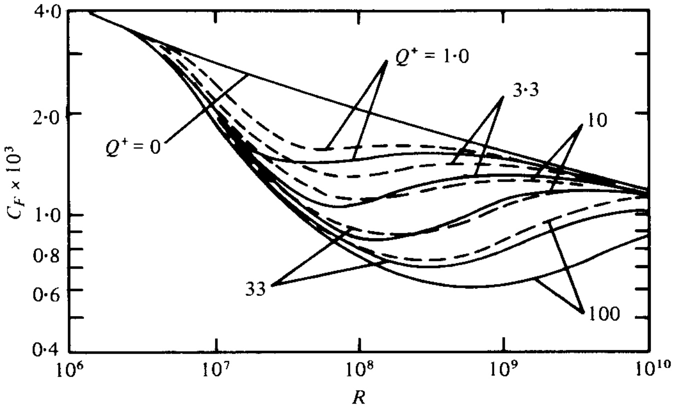

FIGURE 13. Theoretical results, $Q^+$ is the injection flux, the plate length $L = 8·0$ m.

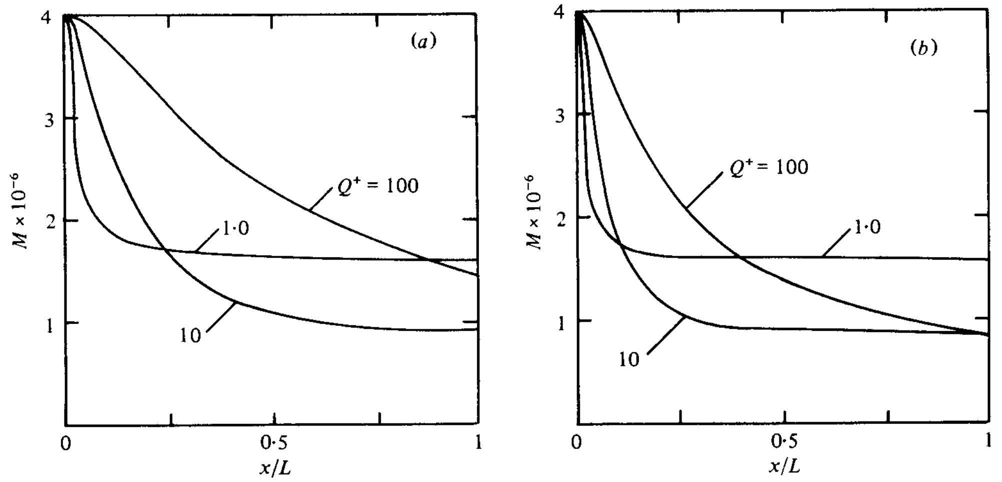

FIGURE 14. The distribution of the mean molecular weight along a plate of length $L = 8·0$ m; $U$ is the free stream velocity. (a) $U$ 20 ms$^{-1}$; (b) $U = 50$ ms$^{-1}$.

concentration are given in figures 15(*a*) and (*b*). Degradation weakly influences the concentration distribution. As $V_*$ changes little along the plate, the value of $M$ is mainly influenced by the distribution of $C$ through $A(C)$. When $C(r_0) \leqslant 3 \times 10^{-5}$, the monotonic decrease of the concentration along the plate and the reduction (through degradation) of the molecular weight quickly reduce the destruction intensity. Thus for $U = 50$ m/s and $Q^+ = 10$ (see figure 16) the degradation practically ceases 1 m from the leading edge and $M$ remains constant $1·6 \times 10^6$ downstream. When $C(r_0) > 3 \times 10^{-5}$, $M$ initially decreases less rapidly because $A(C)$ is smaller, but as $C(x)$ decreases the degradation increases and $M$ falls, tending to a lower downstream limit. The length of the boundary layer in which three is intense degradation increases with $C(r_0)$, while the limiting molecular weight decreases.

Figure 17 shows the variation of the boundary layer thickness along a plate of length 8·0 m for $U = 50$ m/s and various values of $Q^+$. At higher injection fluxes the boundary-layer thickness grows more slowly, although this effect is reduced by degradation.

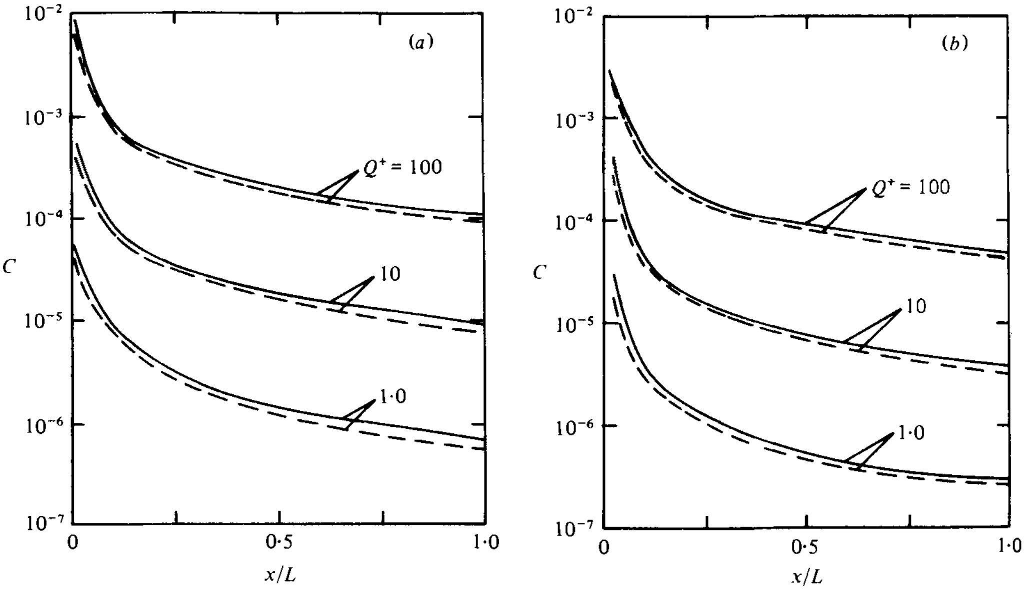

FIGURE 15. Theoretical results of the distribution of the effective concentration along a plate of $L = 8{\cdot}0$ m. (a) $U = 20\ \mathrm{ms}^{-1}$; (b) $U = 50\ \mathrm{ms}^{-1}$.

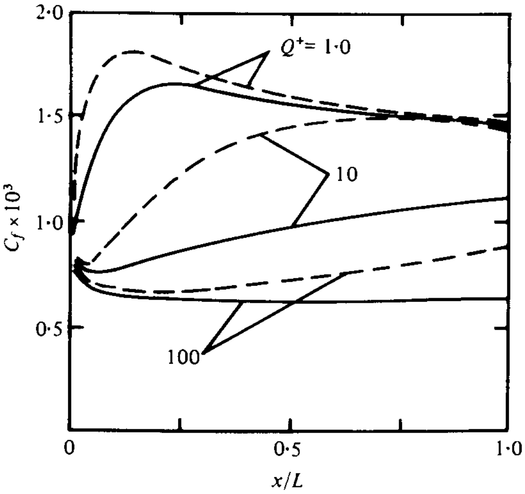

FIGURE 16. The distribution of the local friction coefficient along the plate. $L = 8{\cdot}0$ m, $U = 50\ \mathrm{ms}^{-1}$.

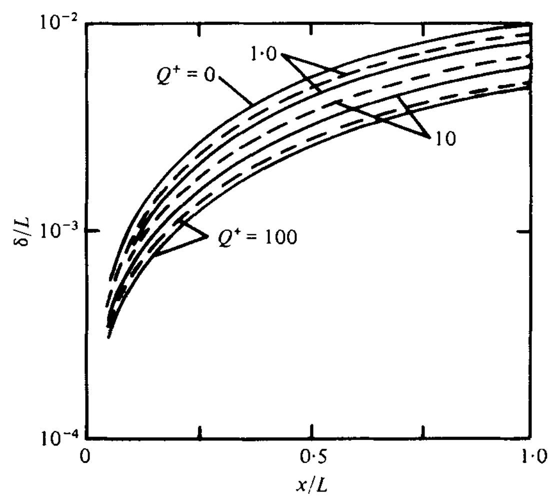

FIGURE 17. The variation of the boundary layer thickness along a plate for different values of the injection flux $Q^+$. $L = 8{\cdot}0$ m, $U = 50\ \mathrm{ms}^{-1}$.

## REFERENCES

BERMAN, N. S. & GEORGE, W. K. 1974 *Phys. Fluids* **17**, 250–251.

BLOCK, H., MORAN, A. N. & WALKER, S. H. 1974 The reduction of turbulent drag and the degradation of poly(styrene) in toluene. *Proc. Int. Conf. Drag Reduct., Cambridge*, pp. 39–50.

COX, L. R., NORTH, A. M. & DUNLOP, E. H. 1974 Evidence for a time-scale effect in drag reduction in solutions of polystyrene in toluene. *Proc. Int. Conf. Drag Reduct., Cambridge*, pp. C2/17–C2/30.

CRAMAIN, PH. & PHILLIPPIDES, PH. 1975 Principaux facteurs physico-chimiques caractérisant l'efficacité des solutions de polymères en reduction de frottement hydrodynamique. *Coll. int. CNRS*, no. 233, pp. 349–355.

GULTER, J. D., ZAKIN, J. L. & PATTERSON, G. K. 1975 *J. Appl. Polymer Sci.* **19**, 3235–3240.

HOYT, J. W. 1966 *Polym. Letters*, **4**, 713–717.

HOYT, J. W. 1972 *Trans. A.S.M.E.* D **94** (2), 1–31.

IOSELEVICH, V. A. & PILIPENKO, V. N. 1973 *Dokl. Akad. Nauk S.S.S.R.* **213**, 808–811; pp. 1266–1269 (in Russian).

IOSELEVICH, V. A. & PILIPENKO, V. N. 1974 *Fluid Dynamics* (*Izv. Akad. Nauk S.S.S.R., Mekhanika Zhidkosti i Gaza*) **9**, no. 1, pp. 47–51.

IVANYUTH, V. F. & CHEKALOVA, L. A. 1976 *Inzhenerno-fizicheskiy Zh.* **31**, 225–230 (in Russian).

KIM, O. K., LITTLE, R. C., PATTERSON, R. L. & TING, R. Y. 1974 *Nature, Lond.* **250**, 408–410.

LUMLEY, J. L. 1969 *Ann. Rev. Fluid Mech.* **1**, 367–384.

MEULEN, J. H. VAN DER 1974 *J. Appl. Sci.* **29**, 161–174.

NAUDASCHER, E. 1972 *Wasserwirtschaft* **62**, (5), 1–13 (in German).

PILIPENKO, V. N. 1975 *Fluid Dynamics* (*Izv. Akad. Nauk S.S.S.R., Mekhanika Zhidkosti i Gaza*) **10**, no. 5, pp. 751–756.

PILIPENKO, V. N. 1977 Simulation of turbulent flows in liquid with polymer additives. In *Turbulentnye techeniya*, pp. 145–150. Moskva: Nauka (in Russian).

POREH, M. J. 1970 *Hydronautics* **4**, (4), pp. 151–155.

RAM ARIE A. 1975 Polymers and their effectiveness in drag reduction. *Coll. Int. CNRS*, no. 233, pp. 271–280 (Discussion).

SEDOV, L. I., IOSELEVICH, V. A. & PILIPENKO, V. N. 1977 Friction and heat transfer in near wall flows with polymer additives. In *Turbulentnye techeniya*, pp. 7–9. Moskva: Nauka (in Russian).

SEDOV, L. I., VASETSKAYA, N. G. & IOSELEVICH, V. A. 1974 Calculation of turbulent boundary layers with polymer additives. *Proc. Int. Conf. Drag Reduct., Cambridge*, pp. B6/69–B6/88.

SELLIN, R. H. J. 1974 Experiments with polymer additives in a long pipe line. *Proc. Int. Conf. Drag Reduct., Cambridge*, pp. G219–G230 (discussion, pp. G47–G54).

SHIN, H. 1965 Sc.D. Thesis, MIT, chem. Eng. Dept.

SPANGLER, J. G. 1969 Studies of viscous drag reduction with polymers including turbulence measurements and roughness effects. In *Viscous Drag Reduction*, pp. 131–157. New York.

VASETSKAYA, N. G. & IOSELEVICH, V. A. 1970 *Fluid Dynamics* (*Izv. Akad. Nauk S.S.S.R., Mekhanika Zhidkosti i Gaza*) **5**, no. 2, pp. 289–296.

VIRK, P. S. 1971 *J. Fluid Mech.* **45**, 225–246.

VIRK, P. S. 1975 *A.I.C.hE. J.* **21**, 256–656.

VIRK, P. S., MERRILL, E. W., MICKLEY, H. S. & SMITH, K. A. 1966 The critical wall shear stress for reduction of turbulent drag in pipe flows by polyethylene oxides in dilute solution. In *Modern Developments in the Mechanics of Continua* (ed. S. Esckinazi). New York: Academic Press.

VIRK, P. S., MERRILL, E. W., MICKLEY, H. S. & SMITH, K. A. 1967 *J. Fluid Mech.* **30**, 305–328.

VIRK, P. S. & MERRILL, E. W. 1969 The onset of dilute polymer solution phenomena. In *Viscous Drag Reduction*, pp. 107–130. New York: Plenum.